Two-particle Schrödinger equation animations of wave packet–wave packet scattering

Jon J. V. Maestri[a)] and Rubin H. Landau[b)]
Oregon State University, Department of Physics, Corvallis, Oregon 97331

Manuel J. Páez
Department of Physics, University of Antioquia, Medellin, Colombia

A simple and explicit technique for the numerical solution of the two-particle, time-dependent Schrödinger equation is assembled and tested. The technique can handle interparticle potentials that are arbitrary functions of the coordinates of each particle, arbitrary initial and boundary conditions, and multidimensional equations. Plots and animations are given here and on the World Wide Web of the scattering of two wave packet in one dimension. © *2000 American Association of Physics Teachers.*

I. INTRODUCTION

Rather than showing the time dependence of two particles interacting with each other, quantum mechanics textbooks often present a time-independent view of a single particle interacting with an external potential. In part, this makes the physics clearer, and in part, this reflects the difficulty of solving the time-independent two-particle Schrödinger equation for the motion of wave packets. In the classic quantum mechanics text by Schiff,[1] examples of realistic quantum scattering, such as that in Fig. 1, are produced by computer simulations of wave packets colliding with square potential barriers and wells. Generations of students have carried memories of these images (or of the film loops containing these frames[2]) as to what realistic quantum scattering looks like.

While Fig. 1 is a good visualization of a quantum scattering process, we wish to extend simulations of realistic quantum interactions to include particle–particle scattering when both particles are represented by wave packets. Although more complicated, this, presumably, is closer to nature and may illustrate some physics not usually found in quantum mechanics textbooks. In addition, our extension goes beyond the treatment found in most computational physics texts which concentrate on *one-particle* wave packets,[3–5] or highly restricted forms of *two-particle* wave packets.[6]

The simulations of the time-dependent Schrödinger equation shown by Schiff were based on the 1967 finite-difference algorithms developed by Goldberg, Schey, and Schwartz.[2] Those simulations, while revealing, had problems with stability and probability conservation. A decade later, Cakmak and Askar[7] solved the stability problem by using a better approximation for the time derivative. After yet another decade, Visscher[8] solved the probability conservation problem by solving for the real and imaginary parts of the wave function at slightly different (''staggered'') times.

In this paper we combine the advances of the last 20 years and extend them to the numerical solution of the *two-particle*—in contrast to the *one-particle*—time-dependent Schrödinger equation. Other than being independent of spin, no assumptions are made regarding the functional form of the interaction or initial conditions, and, in particular, there is no requirement of separation into relative and center-of-mass variables.[6] The method is simple, explicit, robust, easy to modify, memory preserving, and may have research applications. However, high precision does require small time and space steps, and, consequently, long running times. A similar approach for the time-dependent one-particle Schrödinger equation in a two-dimensional space has also been studied.[5]

II. TWO-PARTICLE SCHRÖDINGER EQUATION

We solve the two-particle time-dependent Schrödinger equation

$$i \frac{\partial}{\partial t} \psi(x_1, \ x_2, t) = H \psi(x_1, \ x_2, t), \tag{1}$$

$$H = -\frac{1}{2m_1} \frac{\partial^2}{\partial x_1^2} - \frac{1}{2m_2} \frac{\partial^2}{\partial x_2^2} + V(x_1, x_2), \tag{2}$$

where, for simplicity, we assume a one-dimensional space and set $\hbar = 1$. Here H is the Hamiltonian operator and m_i and x_i are the mass and position of particle $i = 1,2$. Knowledge of the two-particle wave function $\psi(x_1, \ x_2, t)$ permits the calculation of the probability density for particle 1 being at x_1 and particle 2 being at x_2 at time t:

$$\rho(x_1, \ x_2, t) = |\psi(x_1, \ x_2, t)|^2. \tag{3}$$

The fact that particles 1 and 2 must be located someplace in space leads to the normalization constraint on the wave function:

$$\int_{-\infty}^{+\infty} \int_{-\infty}^{+\infty} dx_1 \, dx_2 |\psi(x_1, \ x_2, t)|^2 = 1. \tag{4}$$

The description of a single particle within a multiparticle system by a single-particle wave function is an approximation unless the system is uncorrelated (in which case the total wave function can be written in product form). However, it is possible to deduce meaningful one-particle densities from the two-particle density by integrating over the other particle:

$$\rho_1(x_i, t) = \int_{-\infty}^{+\infty} dx_j \rho(x_1, \ x_2, t) \quad (i \neq j = 1,2). \tag{5}$$

Here we use a subscript on the single-particle density ρ_i to distinguish it from the two-particle density ρ. Of course, the true solution is $\psi(x_1, \ x_2, t)$, but we find it hard to see the physics in a three-variable complex function, and so, often view $\rho_1(x_1, t)$ and $\rho_2(x_2, t)$ as two separate wave packets colliding.
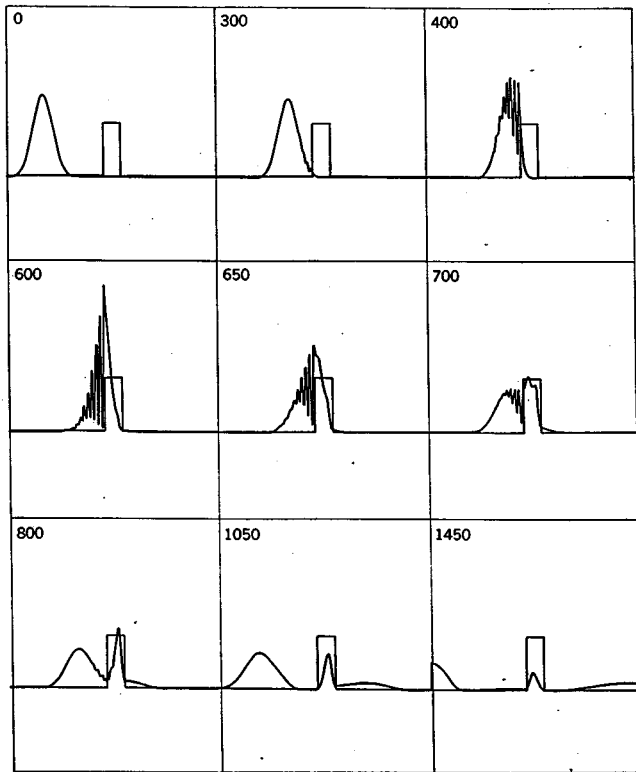
Fig. 1. A time sequence of a Gaussian wave packet scattering from a square barrier as taken from the textbook by Schiff. The mean energy equals the barrier height.

If particles 1 and 2 are identical, then their total wave function should be symmetric or antisymmetric under interchange of the particles. We impose this condition on our numerical solution $\psi(x_1, x_2)$ by forming the combinations

$$\psi'(x_1, x_2) = \frac{1}{\sqrt{2}} [\psi(x_1, x_2) \pm (x_2, x_1)] \Rightarrow \qquad (6)$$

$$2\rho(x_1, x_2) = |\psi(x_1, x_2)|^2 + |\psi(x_2, x_1)|^2$$
$$\pm 2 \operatorname{Re}[\psi^*(x_1, x_2)\psi(x_2, x_1)]. \qquad (7)$$

The cross term in (7) places an additional correlation into the wave packets.

III. NUMERICAL METHOD

We solve the two-particle Schrödinger equation (1) via a finite difference method that converts the partial differential equation into a set of simultaneous, algebraic equations. First, we evaluate the dependent variable ψ on a grid of discrete values for the independent variables:[2]

$$\psi(x_1, x_2, t) = \psi(x_1 = l\Delta x_1, x_2 = m\Delta x_2, t = n\Delta t) \equiv \psi_{l,m}^n, \qquad (8)$$

where l, m, and n are integers. The space part of the algorithm is based on Taylor expansions of $\psi(x_1, x_2, t)$ in both the x_1 and x_2 variables up to $\mathcal{O}(\Delta x^4)$, for example,

$$\frac{\partial^2 \psi}{\partial x_1^2} \simeq \frac{\psi(x_1 + \Delta x_1, x_2) - 2\psi(x_1, x_2) + \psi(x_1 - \Delta x_1, x_2)}{\Delta x_1^2}$$
$$+ \mathcal{O}(\Delta x_1^2). \qquad (9)$$

In discrete notation, the right-hand side of the Schrödinger equation (1) now becomes

$$H\psi = -\frac{\psi_{l+1,m} - 2\psi_{l,m} + \psi_{l-1,m}}{2m_1 \Delta x_1^2}$$
$$- \frac{\psi_{l,m+1} - 2\psi_{l,m} + \psi_{l,m-1}}{2m_2 \Delta x_2^2} + V_{lm}\psi_{l,m}. \qquad (10)$$

Next, we express the time derivative in (1) in terms of finite time differences by taking the formal solution to the time-dependent Schrödinger equation and making a forward-difference approximation for the time evolution operator:

$$\psi_{l,m}^{n+1} = e^{-i\Delta tH}\psi_{l,m}^n \simeq (1 - i\Delta tH)\psi_{l,m}^n. \qquad (11)$$

Although simple, this approximation scheme is unstable since the term multiplying ψ has eigenvalue $(1 - iE\Delta t)$ and modulus $\sqrt{1 + E^2 \Delta t^2}$, and this means the modulus of the wave function increases with each time step.[3] The improvement introduced by Askar and Cakmak[7] is a central difference algorithm also based on the formal solution (11):

$$\psi_{l,m}^{n+1} - \psi_{l,m}^{n-1} = (e^{-i\Delta tH} - e^{i\Delta tH})\psi_{l,m}^n \cong -2i\Delta tH\psi_{l,m}^n, \qquad (12)$$

$$\Rightarrow \psi_{l,m}^{n+1} \simeq \psi_{l,m}^{n-1} - 2i\left[\left\{\left(\frac{1}{m_1} + \frac{1}{m_2}\right)4\lambda + \Delta x V_{l,m}\right\}\psi_{l,m}^n \right.$$
$$- \lambda\left\{\frac{1}{m_1}(\psi_{l+1,m}^n + \psi_{l-1,m}^n)\right.$$
$$\left.\left. + \frac{1}{m_2}(\psi_{l,m+1}^n + \psi_{l,m-1}^n)\right\}\right], \qquad (13)$$

where we have assumed $\Delta x_1 = \Delta x_2$ and formed the ratio $\lambda = \Delta t / \Delta x^2$.

Equation (13) is an *explicit* solution in which the wave function at only two past time values must be stored simultaneously in memory to determine all future times by continued iteration. In contrast, an *implicit* solution determines the wave function for all future times in just one step, yet this one step requires the solution of simultaneous algebraic equations involving all space and time values. Accordingly, an implicit solution requires the inversion of exceedingly large matrices.

While the explicit method (13) produces a solution which is stable and second-order accurate in time, in practice it does not conserve probability well. Visscher[8] has deduced an improvement which takes advantage of the extra degree of freedom provided by the complexity of the wave function to preserve probability better. If we separate the wave function into real and imaginary parts,

$$\psi_{l,m}^{n+1} = u_{l,m}^{n+1} + iv_{l,m}^{n+1}, \qquad (14)$$

the algorithm (13) separates into the pair of coupled equations:

$$u_{l,m}^{n+1} = u_{l,m}^{n-1} + 2\left[\left\{\left(\frac{1}{m_1} + \frac{1}{m_2}\right)4\lambda + \Delta t V_{l,m}\right\}v_{l,m}^{n}\right.$$

$$-\lambda\left\{\frac{1}{m_1}(v_{l+1,m}^{n} + v_{l-1,m}^{n})\right.$$

$$\left.\left. + \frac{1}{m_2}(v_{l,m+1}^{n} + v_{l,m-1}^{n})\right\}\right], \quad (15)$$

$$v_{l,m}^{n+1} = v_{l,m}^{n-1} - 2\left[\left\{\left(\frac{1}{m_1} + \frac{1}{m_2}\right)4\lambda + \Delta t V_{l,m}\right\}u_{l,m}^{n}\right.$$

$$-\lambda\left\{\frac{1}{m_1}(u_{l+1,m}^{n} + u_{l-1,m}^{n})\right.$$

$$\left.\left. \times \frac{1}{m_2}(u_{l,m+1}^{n} + u_{l,m-1}^{n})\right\}\right]. \quad (16)$$

Visscher's advance evaluates the real and imaginary parts of the wave function at slightly different (staggered) times,

$$[u_{l,m}^{n}, v_{l,m}^{n}] = [\text{Re}\,\psi(x,t), \text{Im}\,\psi(x, t + \tfrac{1}{2}\Delta t)], \quad (17)$$

and uses a definition for probability density that differs for integer and half-integer time steps,

$$\rho(x,t) = |\text{Re}\,\psi(x,t)|^2 + \text{Im}\,\psi\left(x, t + \frac{\Delta t}{2}\right)\text{Im}\,\psi\left(x, t - \frac{\Delta t}{2}\right), \quad (18)$$

$$\rho\left(x, t + \frac{\Delta t}{2}\right) = \text{Re}\,\psi(x, t + \Delta t)\text{Re}\,\psi(x,t)$$

$$+ \left|\text{Im}\,\psi\left(x, t + \frac{\Delta t}{2}\right)\right|^2. \quad (19)$$

These definitions reduce to the standard one for infinitesimal Δt, and provide an algebraic cancellation of errors so that probability is conserved.

IV. SIMULATIONS

We assume that the particle–particle potential is central and depends only on the relative distance between particles 1 and 2 (the method can handle any x_1 and x_2 functional dependencies). We have investigated a ''soft'' potential with a Gaussian dependence, and a ''hard'' one with a square-well dependence, both with range α and depth V_0:

$$V(x_1, x_2) = \begin{cases} V_0 \exp\left[-\dfrac{|x_1 - x_2|^2}{2\alpha^2}\right] & \text{(Gaussian)} \\ V_0\,\theta(\alpha - |x_1 - x_2|) & \text{(square)} \end{cases}. \quad (20)$$

A. Initial and boundary conditions

We model a scattering experiment in which particle 1, initially at x_1^0 with momentum k_1, collides with particle 2, initially far away at x_2^0 with momentum k_2, by assuming a product of independent wave packets for particles 1 and 2:

$$\psi(x_1, x_2, t=0) = e^{ik_1 x_1}\exp\left[-\frac{(x_1 - x_1^0)^2}{4\sigma^2}\right]$$

$$\times e^{ik_2 x_2}\exp\left[-\frac{(x_2 - x_2^0)^2}{4\sigma^2}\right]. \quad (21)$$

Table I. Parameters for the antisymmetrized, $m-m$ collision with an attractive square well potential.

Parameter	Value
Δx	0.001
Δt	2.5×10^{-7}
k_1	$+157$
k_2	-157
σ	0.05
x_1^0	467 (0.33×1401 steps)
x_2^0	934 (0.667×1401 steps)
$N_1 = N_2$	1399
L	1.401 (1401 space steps)
T	0.005 (20 000 time steps)
V_0	$-100\,000$
α	0.062

Because of these Gaussian factors, ψ is not an eigenstate of the particle i momentum operators $-i\partial/\partial x_i$, but instead contains a spread of momenta about the mean, initial momenta k_1 and k_2. If the wave packet is made very broad ($\sigma \to \infty$), we would obtain momentum eigenstates. Note that while the Schrödinger equation may separate into one equation in the relative coordinate x and another in the center-of-mass coordinate X, the initial condition (21), or more general ones, cannot be written as a product of separate functions of x and X. Accordingly, a solution of the partial differential equation in two variables is required.[6]

We start the staggered-time algorithm with the real part of wave function (21) at $t=0$ and the imaginary part at $t = \Delta t/2$. The initial imaginary part follows by assuming that $\Delta t/2$ is small enough, and σ large enough, for the initial time dependence of the wave packet to be that of the plane wave parts:

$$\text{Im}\,\psi\left(x_1, x_2, t = \frac{\Delta t}{2}\right)$$

$$\simeq \sin\left[k_1 x_1 + k_2 x_2 - \left(\frac{k_1^2}{2m_1} + \frac{k_2^2}{2m_2}\right)\frac{\Delta t}{2}\right]$$

$$\times \exp-\left[\frac{(x_1 - x_1^0)^2 + (x_2 - x_2^0)^2}{2\sigma^2}\right]. \quad (22)$$

In a scattering experiment, the projectile enters from infinity and the scattered particles are observed at infinity. We model that by solving our partial differential equation within a box of side L (ideally) much larger than both the range of the potential and the width of the initial wave packet. This leads to the boundary conditions

$$\psi(0, x_2, t) = \psi(x_1, 0, t) = \psi(L, x_2, t) = \psi(x_1, L, t) = 0. \quad (23)$$

The largeness of the box minimizes the effects of the boundary conditions during the collision of the wave packets, although at large times there will be interesting, yet artificial, collisions with the walls of the box.

Some typical parameters used in our tests are given in Table I (the code with sample files are available on the Web[9]). Our space step size $\Delta x = 0.001$ is 1/1400th of the size of the box L, and 1/70th of the size ($\sqrt{2\sigma} \simeq 0.07$) of the wave packet. Our time step $\Delta t = 2.5 \times 10^{-7}$ is 1/20 000th of the total time T, and 1/2000th of a typical time for the wave packet $[2\pi/(k_1^2/2m_1) \simeq 5 \times 10^{-4}]$. In all cases, the potential
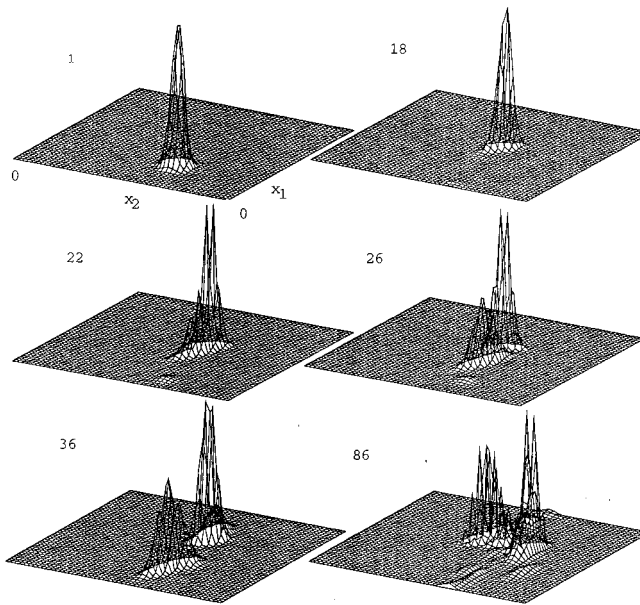
Fig. 2. Six frames from an animation of the two-particle density $\rho(x_1, x_2, t)$ as a function of the position of particle 1 with mass m and of the position of particle 2 with mass $10m$. This same collision is described in Fig. 3 by showing separate plots of the more common single-particle densities $\rho(x_1, t)$ and $\rho(x_2, t)$. In both figures there is a repulsive interaction between the particles and the mean kinetic energy equals twice the barrier height. The numbers in the left-hand corners are the times in units of $100\Delta t$. Note that each plot ends at the walls of the containing box, and that particle 1 "bounces off" a wall between times 36 and 86 (more evident in Fig. 3).
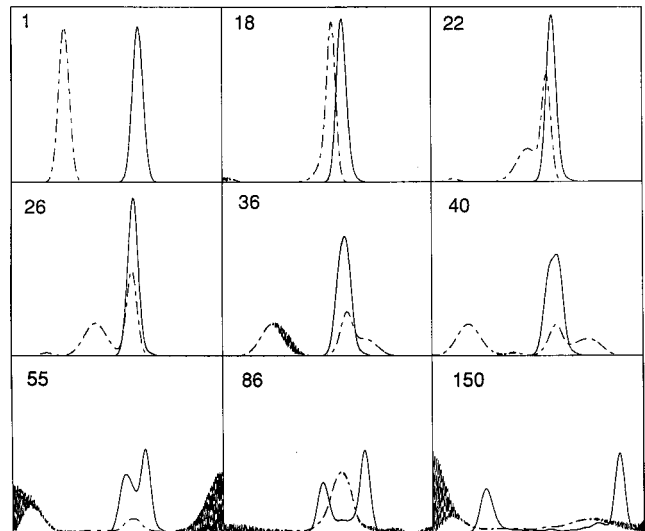

Fig. 3. A time sequence of two Gaussian single-particle wave packets scattering from each other under the influence of a square barrier. The mean kinetic energy equals twice the barrier height. The dashed curve describes particle 1 of mass m and the solid curve particle 2 of mass $10m$. The number in the upper left-hand corner of each frame is the time in units of $100\Delta t$, and the edges of the frames correspond to the walls of the box. Note that at time 55 the wave packet for mass m is seen to be interacting with the wall, as indicated by the interference ripples between incident and reflected waves, and at time 150 the wave packet for mass $10m$ is interacting with the wall (by this time mass m has already had multiple wall interactions).

and wave packet parameters are chosen to be similar to those used in the one-particle studies by Goldberg, Schey, and Schwartz. The time and space step sizes were determined by trial and error until values were found which provided stability and precision (too large a Δx leads to spurious ripples during interactions). In general, stability is obtained by making Δt small enough,[8] with simultaneous changes in Δt and Δx made to keep $\lambda = \Delta t / \Delta x^2$ constant. Total probability, as determined by a double Simpson's-rule integration of (4), is typically conserved to 13 decimal places, impressively close to machine precision. In contrast, the mean energy, for which we do not use a definition optimized to staggered times, is conserved only to 3 places.

B. Barrier-like collisions

We solve our problem in the center-of-momentum system by taking $k_2 = -k_1$ (particle 1 moving to larger x values and particle 2 to smaller x). Our first simulations and Web animations[9,10] emulate the one-particle collisions with barriers and wells studied by Goldberg, Schey, and Schwartz and presented by Schiff. We make particle 2 ten times heavier than particle 1, so that particle 2's initial wave packet moves at 1/10th the speed of particle 1's, and so looks like a barrier. Although we shall describe several scattering events, the animations available on the Web speak for themselves, and we recommend their viewing.

In Fig. 2 we show six frames from an animation of the two-particle density $\rho(x_1, x_2, t)$ as a simultaneous function of the particle positions x_1 and x_2. In Fig. 3 we show, for this same collision, the *single-particle* densities $\rho_1(x = x_1, t)$ and $\rho_2(x = x_2, t)$ extracted from $\rho(x_1, x_2, t)$ by in-

tegrating out the dependence on the other particle via (5). Since the mean energy equals twice the maximum height of the potential barrier, we expect complete penetration of the packets, and indeed, at time 18 we see that the wave packets have large overlap, with the repulsive interaction "squeezing" particle 2 (it gets narrower and taller). During times 22–40 we see part of wave packet 1 reflecting off wave packet 2 and then moving back to smaller x (the left). From times 26 to 55 we also see that a major part of wave packet 1 gets "trapped" inside of wave packet 2 and then leaks out rather slowly.

We see that for times 1–26, the x_2 position of the peak of $\rho(x_1, x_2, t)$ in Fig. 2 changes very little with time, which is to be expected since particle 2 is heavy. In contrast, the x_1 dependence in $\rho(x_1, x_2, t)$ gets broader with time, develops into two peaks at time 26, separates into two distinct parts by time 36, and then, at time 86 after reflecting off the walls, returns to particle 2's position. We also notice in both these figures that at time 40 and thereafter, particle 2 (our "barrier") fissions into reflected and transmitted waves.

As this comparison of Figs. 2 and 3 demonstrates, it seems easier to understand the physics by superimposing two single-particle densities (thereby discarding information on correlations) than by examining the two-particle density. Accordingly, the figures we show hence, and the majority of the animations on the Web, are of single-particle densities.

Figure 3 is similar to the behavior present in Schiff's one-particle simulation, Fig. 1, but without ripples during the collision. Those ripples are caused by interference between scattered and incident waves, and even though we have a square barrier potential acting between the particles, neither
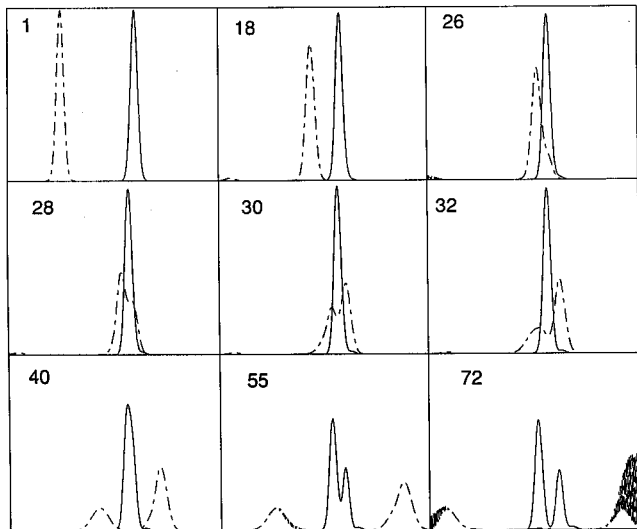
m–10m, Attractive Vsquare

KE = – V/2

Fig. 4. The same as Fig. 3, except now the potential is attractive with the mean energy equal to half the depth.
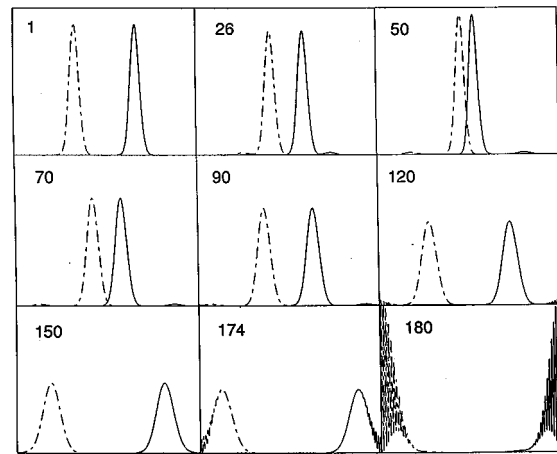
m–m, Repulsive Vsquare

KE = +V/4

Fig. 5. The same as Fig. 4, except now for a repulsive $m-m$ collision in which the mean energy equals one-quarter of the barrier's height.

particle ''feels'' the discontinuity of the sharp potential edge at any one time. However, there are ripples when our wave packets hit the walls, as seen at times 55 and 150.

At early times in Fig. 3, as well as in other animations, we can see very small wave packets moving in opposite directions to the larger wave packets for each particle. These are numerical artifacts. While wave packets with reversed values of k are valid solutions of the Schrödinger equation, they should be eliminated by the initial conditions. For example, if $\exp(ikx)$ is a valid solution, then so is $\exp(-ikx)$, yet it is hard to get rid of it completely.[11]

Something new in Fig. 3, that is not in Schiff, is the delayed fission of the heavier particle's wave packet after time 40 into transmitted and reflected waves (it occurred earlier for the lighter particle). In addition, at time 86 we see that the reflected and transmitted parts of the wave packet of particle 1 have reconstituted themselves into a single but broadened wave packet, and that at time 150 it is again being reflected from the left wall. (Although it may be somewhat confusing to keep looking at the interaction after reflections from the artificial bounding box, we display it in order to show some of the interesting physics uncovered.)

In Fig. 4 we see another $m-10m$ collision. This time there is an attractive interaction between the particles and again the mean energy equals half the well depth. Even though the kinetic energy is low, the interaction is attractive and so particle 1 passes through particle 2. However, some of wave packet 1 is reflected back to the left after the collision, and, as we see at time 55, the wave packet for the heavy particle 2 fissions (presumably) as a consequence of its attraction to the two parts of wave packet 1.

Although we do not show them here, on the Web we also display movies of collisions corresponding to a Gaussian potential acting between the particles. These are much softer collisions and have behaviors similar to classical particles bouncing off each other, with squeezing and broadening of the wave packets, but little breakup or capture.

C. $m-m$ collisions

In Fig. 5 we show nine frames from the movie of a repulsive $m-m$ collision in which the mean kinetic energy equals one-quarter of the barrier height. The initial packets are seen to slow down as they approach each other, with their mutual repulsion narrowing and raising the packets up until the time (50) when they begin to bounce back. The wave packets at still later times are seen to retain their shape, with a progressive broadening until they collide with the walls and break up. As shown on the Web, when the mean energy is raised there will be both transmitted and reflected waves, already seen in Fig. 3 for an $m-10m$ collision.

In Fig. 6 we show nine frames from the movie of an attractive $m-m$ collision in which the mean energy equals one-quarter of the well depth. The initial packets now speed up as they approach each other, and at time 60 the centers

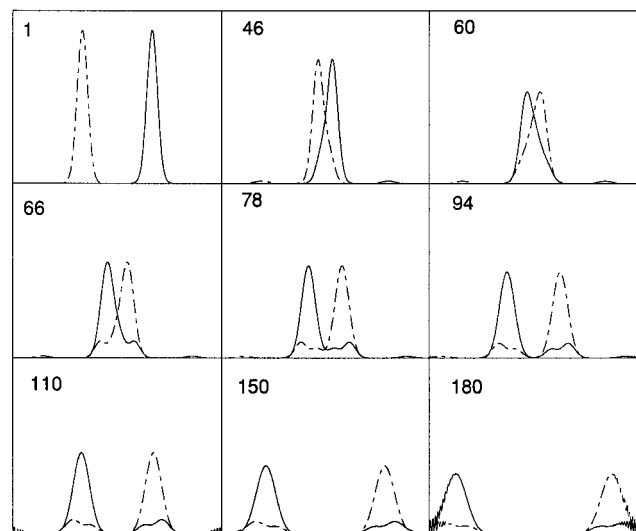## m–m, Attractive Vsquare

KE = – V/4

Fig. 6. The same as Fig. 4, except now for an attractive $m-m$ collision in which the mean energy equals one-quarter of the well's depth.

Antisymmetrized m–m, Attractive Vsquare
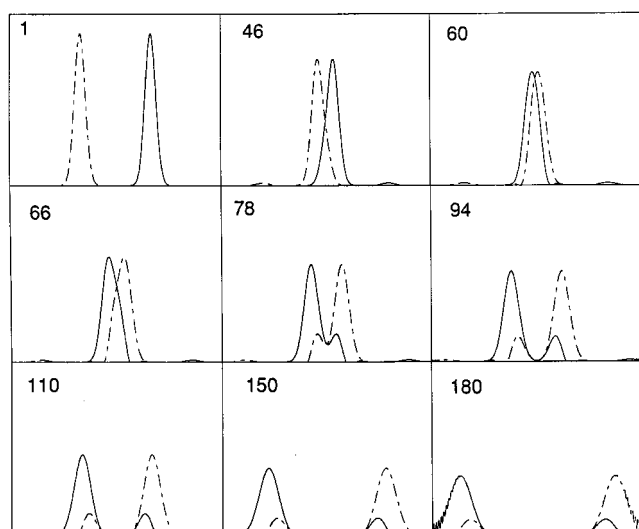
KE = – V/4

Fig. 7. The same as Fig. 4, except now for an attractive $m-m$ collision in which the mean energy equals one-quarter of the well's depth, and for which the wave function has been antisymmetrized.

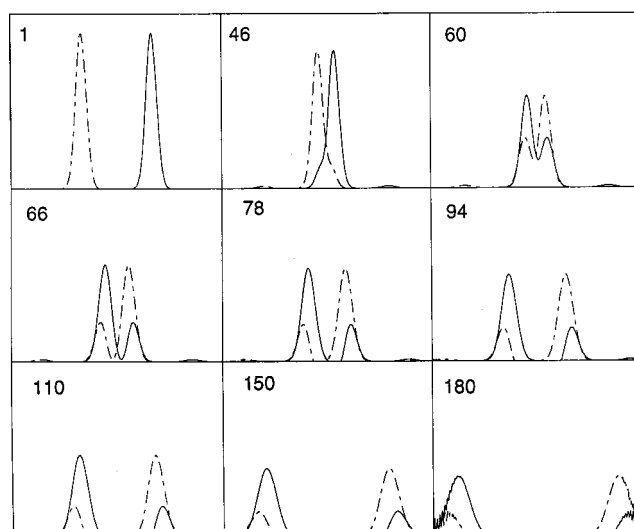## Symmetrized m–m, Attractive Vsquare

KE = –V/4

Fig. 8. The same as Fig. 4, except now for an attractive $m-m$ collision in which the mean energy equals one-quarter of the depth, and for which the wave function has been symmetrized.

have already passed through each other. After that, a transmitted and reflected wave for each packet is seen to develop (times 66–78). Although this may be just an artifact of having two particles of equal mass, from times 110 to 180 we see that each packet appears to capture or ''pick up'' a part of the other packet and move off with it.

In Fig. 7 we repeat the collision of Fig. 6, only now for a wave function that has been *antisymmetrized* according to (7). The antisymmetrization is seen to introduce an effective repulsion into what is otherwise an attraction (compare the two figures for times 60–66). Again, some capture of the other wave packet is noted from times 94 on, only now the internal captured wave packet retains its Gaussian-like shape, apparently the result of decreased interference.

Finally, in Fig. 8 we repeat the collisions of Figs. 6 and 7, only now for a wave function that has been *symmetrized* according to (7). The symmetrization is seen to introduce an effective added attraction (compare the three figures for time 60, which shows the greatest penetration for the symmetrized case). While there is still capture of the other wave packet, the movie gives the clear impression that the wave packets interchange with each other as a consequence of the symmetrization (Fig. 8).

V. SUMMARY AND CONCLUSIONS

We have assembled and tested a general technique for the numerical solution of the two-particle, time-dependent Schrödinger equation. Because the technique is general, application to two or three dimensions and for other potentials and initial conditions should be straightforward. For example, further studies may want to investigate initial conditions corresponding to bound particles interacting with a surface, or the formation of a molecule near a surface.

The Goldberg–Schiff image (Fig. 1) of a wave packet interacting with a potential barrier is still a valuable model for understanding the physics occurring during a particle's collision. Here we have extended the level of realism to what a collision between two particles looks like. In doing so with a simple square-well potential between the two particles, we have discovered that fission of the initial single-particle wave packets into transmitted and reflected waves occurs quite often, and that the transmitted packet of one particle often moves off with the reflected packet of the other as if they were bound. While somewhat of a challenge to understand fully, we have also provided animations of the behavior of the two-particle density during collisions. We have placed the animations, source codes, and movie-making instructions on the Web with the hope that future students will also carry some of these images of the quantum world with them.

[a] Present address: CH2M Hill, P.O. Box 428, Corvallis, OR 97330.

[b] Electronic mail: rubin@physics.orst.edu; http://www.physics.orst.edu/~rubin

[1] L. I. Schiff, *Quantum Mechanics* (McGraw–Hill, New York, 1968), 3rd ed., p. 106.

[2] A. Goldberg, H. M. Schey, and J. L. Schwartz, ''Computer-Generated Motion Pictures of One-Dimensional Quantum-Mechanical Transmission and Reflection Phenomena,'' Am. J. Phys. **35**, 177–186 (1967).

[3] S. E. Koonin, *Computational Physics* (Benjamin, Menlo Park, 1986), pp. 176–178.

[4] N. J. Giordano, *Computational Physics* (Prentice–Hall, Upper Saddle River, NJ, 1997), pp. 280–289.

[5] R. H. Landau and M. J. Paez, *Computational Physics, Problem Solving*

With Computers (Wiley, New York, 1997), pp. 399–408.

[6] S. Brandt and H. D. Dahmen, *Quantum Mechanics on the Personal Computer* (Springer-Verlag, Berlin, 1990), Chap. 5, pp. 82–92.

[7] A. Askar and A. S. Cakmak, ''Explicit Integration Method for the Time-Dependent Schrödinger Equation for Collision Problems,'' J. Chem. Phys. **68**, 2794–2798 (1978).

[8] P. B. Visscher, ''A Fast Explicit Algorithm for the Time-Dependent Schrödinger Equation,'' Comput. Phys. **5**, 596–598 (Nov/Dec 1991).

[9] *Movies of Wavepacket-Wavepacket Quantum Scattering*, href:// nacphy.physics.orst.edu/ComPhys/PACKETS/

[10] Our movies are animated *gifs* that can be viewed with any Web browser, or viewed and controlled with a movie player such as *Quick Time*. To create them, we have our *C* code *packets.c* output files of wave function data for each time. We plot each data file with the Unix program GNUPLOT to produce one frame, and then convert the plots to gif files. We then use GIFMERGE (Mark Podlipec and Rene K. Mueller 1996, http://www.the-labs.com/GIFMerge/) to merge the frames into an animation. Further information and instructions for making movies using different operating systems and formats can be found on the *Visualization of Scientific Data* section of the Landau Research Group Web pages, http:// nacphy.physics.orst.edu/DATAVIS/datavis.html.

[11] We thank one of the referees for pointing this out to us.

THE DETRITUS OF RELIGIOUS OBFUSCATION

Theologians, incidentally, have contributed nothing. They have invented a world and language of their own, like some mathematicians, but unlike many mathematicians have sought to impose its percepts and precepts on this world. In doing so they have contaminated truth, and wasted the time of those who wish to understand this world. Scientists have had and are continuing to have to scrape away the detritus of religious obfuscation before they can begin their own elucidation.

P. W. Atkins, ''The Limitless Power of Science,'' in *Nature's Imagination—The Frontiers of Scientific Vision*, edited by John Cornwell (Oxford University Press, New York, 1995).